ELSEVIER

Physica C 281 (1997) 159–175

PHYSICA C

New understanding of silver-induced texture in powder-in-tube processed Ag/Bi(2223) tape

Chuanbin Mao [a,1,b,*], Lian Zhou [a], Xiaozu Wu [a], Xiangyun Sun [b]

[a] *Superconducting Material Research Center, Northwest Institute for Nonferrous Metal Research, P.O. Box 71, Baoji Shaanxi 721014, People's Republic of China*

[b] *Materials Science and Engineering Department, Northeastern University, Shengyang 110006, People's Republic of China*

Received 29 July 1996; revised 25 March 1997; accepted 1 April 1997

Abstract

Silver-sheathed bismuth-based $(Bi,Pb)_2Sr_2Ca_2Cu_3O_x$(2223) tape is prepared by the powder-in-tube process from a precursor powder which consists of $(Bi,Pb)_2Sr_2CaCu_2O_x$(2212), $(Ca,Sr)_2PbO_4$, Ca_2CuO_3, CuO, $(Ca,Sr)_{14}Cu_{24}O_{41}$, $Bi_2(Sr,Ca)_2CuO_x$(2201). Silver layers are found to greatly promote the formation and texturing of the 2223 phase. The evidence is defined as silver-induced texture (SIT). The previously defined reaction-induced texture (RIT) for the 2223 phase is also confirmed at the same time. The Pb loss is appreciable due to the removal of the broad silver layers while the Pb loss is negligible when only the lateral layers are removed. X-ray photoelectron spectroscopy (XPS) shows that Pb^{4+} released from Ca_2PbO_4 enters the BiO plane of the 2212 phase to replace Bi^{3+} as Pb^{2+} to make 2223 nucleate. Auger electron spectroscopy (AES) depth profile analysis shows that the oxygen out-diffusion through the silver sheath is very rapid. The mechanism of SIT is proposed to be a combined effect of preventing Pb loss the during high temperature reaction to 2223, supplying a fast out-diffusion path for oxygen produced during 2212 to 2223 transformation, inducing liquid formation to accelerate atomic diffusion, and preferably promoting plate-like grain growth with the a–b plane parallel to the broad layer by a quasi-two-dimensional space. © 1997 Elsevier Science B.V.

Keywords: Silver-induced texture; Reaction-induced texture; Auger electron spectroscopy; X-ray photoelectron spectroscopy; $(Bi,Pb)_2Sr_2Ca_2Cu_3O_x$(2223)

1. Introduction

Texturing of the $(Bi,Pb)_2Sr_2Ca_2Cu_3O_x$(2223) phase is essential to obtain a high-J_c silver-sheathed 2223 tape (Ag/Bi(2223)) by the powder-in-tube (PIT) process. Accordingly, the mechanism of 2223 texture formation must be well understood to monitor the process of preparing technologically interesting composites. So far, many researchers have investigated the texture formation mechanism of the 2223 phase [1–18]. Some earlier authors thought the texturing of 2223 phase is a complex process and related with the combined contribution of deformation, heat treatment and the silver layer [1–3]. Recently, Merchant et al. [4] found that significant texturing of 2223 grains occurred as the 2223 forma-

* Corresponding author. Tel.: +86 917 3382648; fax: +86 917 3382001.

[1] Present address: Materials Science Division, Materials Science and Engineering Department, Tsinghua University, Beijing 100084, People's Republic of China.

PII S0921-4534(97)00148-2

tion reaction took place and thus proposed a reaction-induced texture (RIT) mechanism. In fact, this mechanism has been observed during 2223 phase formation in bulk preparation [5]. More recently, Grasso et al. [6] found that 2212 grains in unreacted Ag/Bi(2223) tapes at the end of the cold-rolling process show already a high degree of texture, which further resulted in a higher average texture of 2223 grains and thereby a higher critical current density of Ag/Bi(2223) tape. Hence they described the mechanism as deformation-induced texture (DIT). Whatever mechanism is described, none of the researchers neglects the role of the silver layer in the formation and texturing of the 2223 phase [1–4,6]. It has been widely believed that Ag positively encourages grain alignment and formation of the 2223 phase [1–4,6–9], but the mechanism by which this occurs is unclear in many aspects. Fortunately, some instructive phenomena have been found:

(1) A trace of liquid formation during 2223 phase formation was observed at the Ag/2223 interface by HRTEM [10].

(2) Studies of the microstructure of the Ag/2223 interface by HRTEM showed that there was no fixed orientation relationship between silver layer and textured 2223 grains [11].

(3) The 2223 phase preferably formed at the Ag/oxide interface and both the density and degree of texture near the Ag/2223 interface were higher than those near the core of the tape [12–14].

(4) There exists a low eutectic point in the Ag–BiPbSrCaCuO system and the existence of silver reduces the melting point of the composite tape by about 10–15° [15–18].

(5) Oxygen diffusion in the silver layer is quick [19,20].

The typical powder-in-tube process begins with the partially reacted powder with 2212 as the main phase (the balancing phases are Ca- or/and Cu-containing phases such as Ca_2PbO_4, CuO, Ca_2CuO_3 to make a nearly 2223 composition). So the formation and texturing of the 2223 phase may develop simultaneously and interact between each other. Kessler et al. thought that the oxygen partial pressure (P_{O_2}) is lowered inside the sheath and thereby the 2223 phase formation is promoted [21]. But they did not consider whether oxygen will be depleted or produced during 2223 phase formation. Considering the oxygen behavior, there are three possibilities for 2223 phase formation in an Ag/Bi(2223) tape:

(1) If the reaction between 2212 and second phases (hereafter denoted as SP for clarity) to form the 2223 phase depletes O_2, i.e.,

$$2212 + SP + O_2 \rightarrow 2223 \quad (1)$$

the lowering of P_{O_2} will not favor the 2223 phase formation.

(2) If the reaction produces O_2, i.e.

$$2212 + SP \rightarrow 2223 + O_2 \quad (2)$$

the lowering of P_{O_2} will accelerate the 2223 phase formation.

(3) If the reaction neither deplets nor produces O_2, i.e.

$$2212 + SP \rightarrow 2223 \quad (3)$$

the 2223 phase formation will not be related to P_{O_2}.

In fact, the 2223 phase formation in the Ag/Bi(2223) tape is strongly dependent on P_{O_2} [21]. There exists an optimal P_{O_2} for the 2223 phase formation in the Ag/Bi(2223) tape at a fixed temperature [21]. For example, the optimal P_{O_2} is 6×10^3 Pa at $T = 830$°C (lower than P_{O_2} in air). Under this condition, the 2223 phase content was higher than 80% after the tape was sintered for 20 h, while the tape sintered in air for 20 h contained only 2% 2223 phase. So above case (3) will not be possible. Zhu et al. [22] thought that it was case (2) that really happened. So it is essential to clarify the oxygen behavior when considering the effect of the silver layer on the texture growth of the 2223 phase.

Many experiments [23–25] have shown that J_c is the largest in the layer near the silver sheath due to the better microstructure. Larbalestier et al. [23] found that across the width of the Ag/Bi-2223 tape the J_c of the middle strip is about 3–5 times smaller than that of the side strips due to the better alignment and phase purity at the sides of the tape than in the center. Lelovic et al. [24] demonstrated that across the thickness of the Ag/Bi-2223 tapes, there is also an inhomogeneity of J_c. A layer about 10 μm thick adjacent to the broad silver layer can transport current density as high as 1.1×10^5 A/cm^2 at 77 K and zero applied field. Welp et al. [25] recently obtained a high J_c (77 K, 0 T) up to 8×10^4 A/cm^2 in a 2–3 μm thick layer close to the silver sheath where the highly textured monophasic 2223 phase exists, by magneto-optical imaging technique to map spatial

variation. These results firmly confirm that the silver sheath, not only its broad layers but also its lateral layers, contributes to the formation and texturing of the 2223 phase.

To make further understanding of the role of the silver layer for texturing and formation of the 2223 phase, we investigate the effect of the broad and lateral silver layers on the texture growth of the 2223 phase and the oxygen behavior during the 2223 phase formation.

2. Experimental details

2.1. Preparation of Ag / Bi(2223) tape

The standard PIT process was used to prepare a silver-sheathed Bi(2223) composite tape. The precursor powder was prepared by oxalate coprecipitation with the nominal composition of $Bi_{1.8}Pb_{0.4}Sr_{2.0}Ca_{2.2}Cu_{3.06}O_x$. After the oxalate precursor had been calcined at 800°C for 20 h, BiPbSrCaCuO powder was obtained with main phase compositions of $(Bi,Pb)_2Sr_2Ca_1Cu_2O_x$(2212), $(Ca,Sr)_2PbO_4$, CuO and minor phase compositions of Ca_2CuO_3, $(Ca,Sr)_{14}Cu_{24}O_{41}$, $(Bi,Pb)_2Sr_2CuO_x$(2201). The as-ground powder (in argon) was packed into a silver tube (I.D. = 6.9 mm, O.D. = 9.8 mm) in argon, and the tube was sealed with copper columns. Then it was swaged and drawn into wire (O.D. = 1.4 mm).

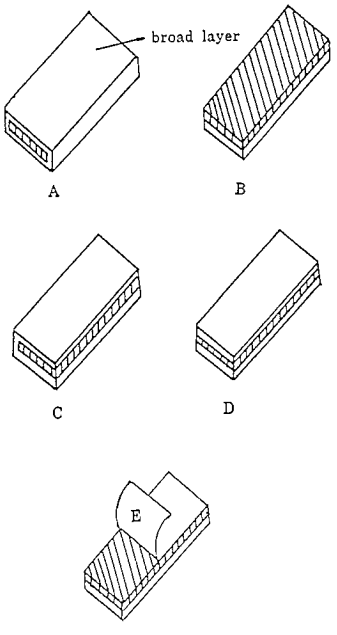

Fig. 1. Schematic illustration of the sample with different silver layer configurations; for details about A–D see text, E indicates the position where AES was done.

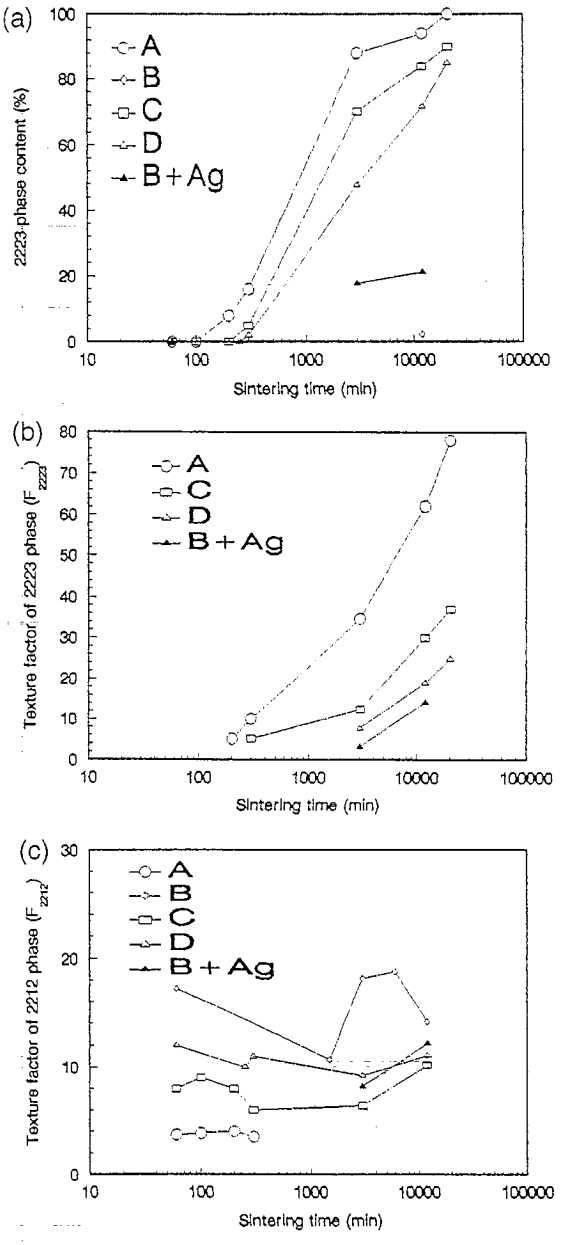

Fig. 2. Heat treatment time dependences of (a) f_{2223}, (b) F_{2223} and (c) F_{2212}.

The wire was further cold-rolled into thin tape (0.15 mm in thickness and 4 mm in width) in two passes. The superconducting cores were typically 3 mm wide and 80 μm thick.

2.2. Preparation of composite tape with different silver layer configurations

Tens of short samples (~ 3 cm in length) were cut from the above as-rolled long tape, and the samples with different silver layer configurations were prepared as follows:

(1) As-rolled tape (group A), the broad surface of the oxide layer was labelled as A.

(2) Both lateral silver layers were cut longitudinally until the black powder had just been exposed, and then the silver layer on one broad surface of the tape was peeled (group B). The so-exposed wide surface of the oxide layer was labelled as B and the counter surface of the oxide layer, namely Ag/oxide interface, was labelled as B + Ag.

(3) One lateral silver layer was cut as (2) (group C), and the non-exposed broad surface of the oxide layer was labelled as C.

(4) Both lateral silver layers were cut as (2) (group D), and the non-exposed broad surface of the oxide layer was labelled as D.

The above configurations and definitions of surfaces of the oxide layers are illustrated in Fig. 1. Each sample was heated at a rate of 1.5°C/min, sintered at 830°C in air for 0–400 h and then quenched to room temperature in air.

2.3. Characterization of sample D

The phase composition and degree of texture of the oxide layer were determined by X-ray diffraction (XRD) on a Rigaku D-S X-ray diffractometer with a Cu target. The silver layer on the wide surface should be peeled off to be subjected to XRD analysis. The 2223 phase content was defined as follows:

$$f_{2223} = I^{0010}_{2223} / \left(I^{0010}_{2223} + I^{008}_{2212} \right) \quad (4)$$

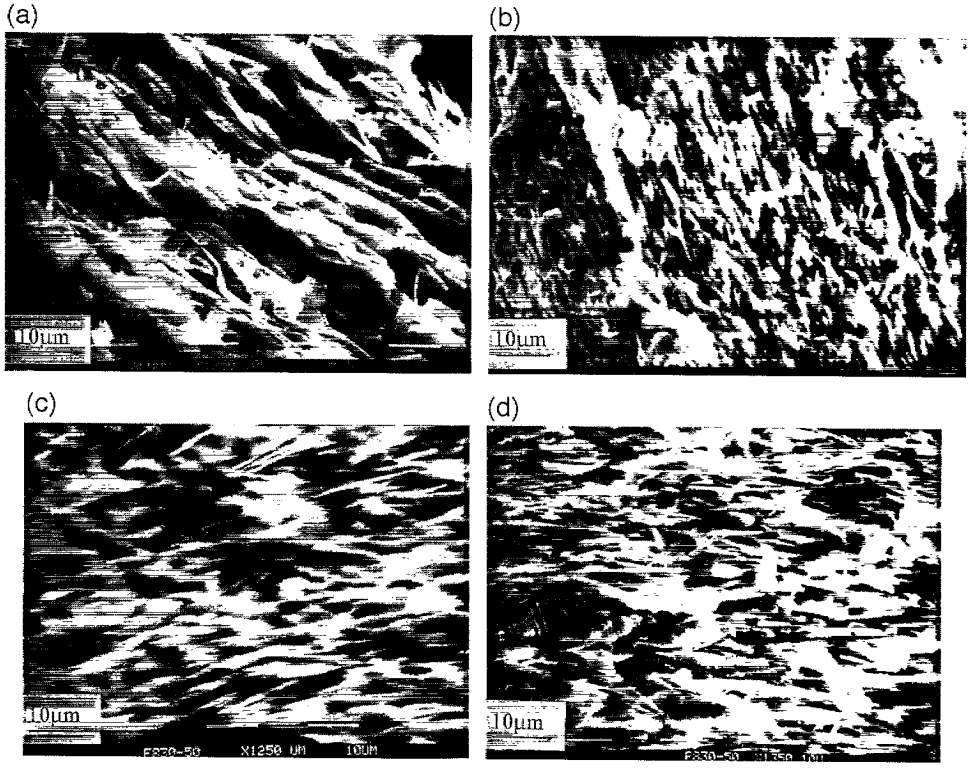

Fig. 3. SEM micrographs of the fractured transverse cross sections of A, B, C, D sintered for 3000 min.

and the degree of texture of the 2223 phase and of the 2212 phase were defined as follows, respectively:

$$F_{2223} = I^{0010}_{2223}/I^{115}_{2223}, \quad (5)$$

$$F_{2212} = I^{008}_{2212}/I^{115}_{2212} \quad (6)$$

where I_x^{hkl} was the integrated intensity of (hkl) reflections of phase x ($x = 2223$ or 2212).

The microstructure of the oxide layer near the core of the tape was observed by scanning electron microscopy (SEM) on a Phillips PSEM-500 SEM coupled with an EDAX system.

Elemental analysis by atomic absorption spectroscopy (AAS) was performed on the powder that was taken as completely as possible from the core of some heat-treated samples.

Auger electron spectroscopy (AES, Perkin Elmer, PHI600 AES Spectrometer) depth profiling measurements were done on the upper peeled silver layer beginning from the Ag/oxide interface as shown in Fig. 1(e). The Ar^+ sputtering speed Z is estimated by the following formula [26]:

$$Z = MSj_p/\rho N_A e \quad (7)$$

where M is the atomic mass of the target, ρ the mass density in kg/cm^3, N_A the Avogadro constant, e the elementary charge (1.6×10^{-9} C), S the sputtering yield in atoms per argon ion, and j_p the density of incident ion beam in A/m^2. In our experiment, j_p is about 0.001 A/m^2 and the target can be regarded as silver ($M = 47$, $\rho = 10482$ kg/m^3), for which S is about 3.5 [27], so we can get $Z \approx 10$ nm/min. To get rid of the black oxide adhered on the internal silver layer surface during peeling, diamond emery paper was used to slightly polish away the black oxide until the white silver surface without obvious black oxides was seen. The surfaces of the cores of the green and sintered tapes of the group A

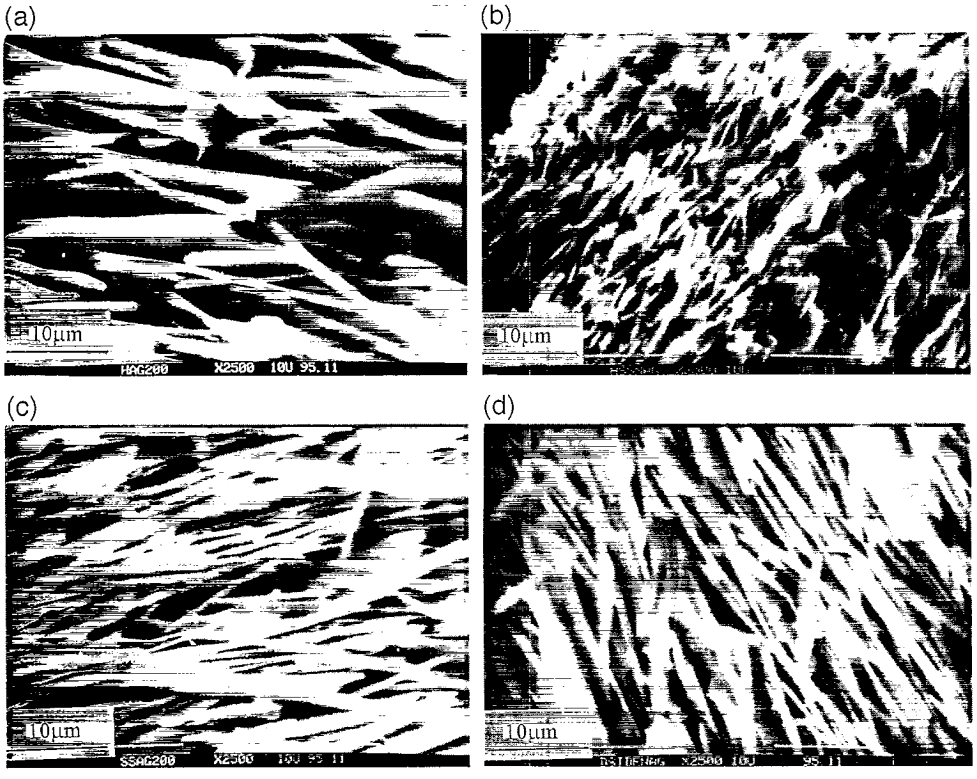

Fig. 4. SEM micrographs of the fractured transverse cross sections of A, B, C, D sintered for 12000 min.

sample were subjected to X-ray photoelectron spectroscopy (XPS, Perkin-Elmer PHI 5400 ESCA system with an Mg target).

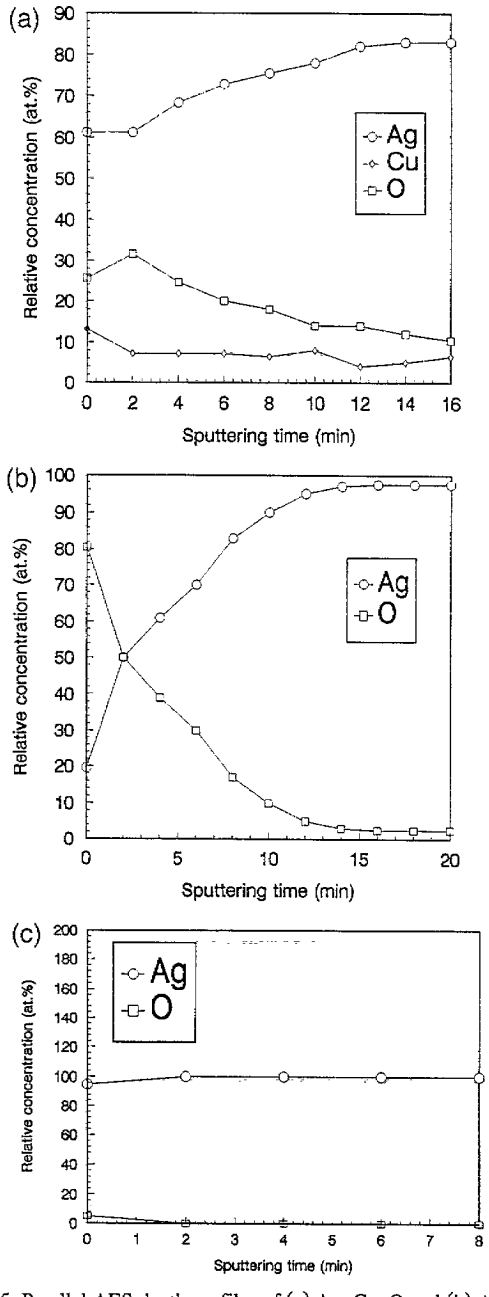

Fig. 5. Parallel AES depth profiles of (a) Ag, Cu, O and (b) Ag, O on the inner broad silver surface in sample A sintered for 1800 min, (c) Ag, O on the outer silver surface of sample A sintered for 1800 min.

3. Results

3.1. XRD characterization

Fig. 2 depicts the heat treatment time dependence of f_{2223}, F_{2223} and F_{2212}, respectively. It should be noted that F_{2212} of sample A and F_{2223} of sample B were not calculated due to the inexistence of the corresponding (115) reflections in the XRD patterns.

It is found that the f_{2223}–t curves of groups A, C, D are all S-shaped, the incubation periods are 100, 200 and 250 min, respectively. The rate of the 2223 phase formation decreases in the sequence of groups A, C, D, B. For sample B, when the sintering time is 20400 min, only $\sim 2\%$ 2223 forms. Moreover, the degree of texture of the 2223 phase increases with the 2223 phase formation, consistent with the RIT mechanism described in Ref. [4]. The rate of the 2223 texture formation also decreases in sequence of groups A, C, D. However, the texture factor for 2212 does not change significantly over the course of the heat treatment which is also consistent with the result in Ref. [4]. Our results show that the texture formation of the 2223 phase is enhanced not only by the silver layer but also by the reaction to form the 2223 phase. The latter is the previously defined reaction-induced texture (RIT) [4]. The former can be defined as a silver-induced texture (SIT). The RIT may come from the preferential growth of oriented 2223 grains [4]. The SIT will be described in Section 4.

3.2. SEM characterization

Figs. 3 and 4 show SEM pictures of the fractured transverse cross sections of samples A, B, C, D sintered for 3000 and 12000 min, respectively. It shows that the degree of texture of the 2223 phase increases with time for each group (A, C, D), and the degree of texture decreases in the sequence of A, C, D at a fixed time, which is consistent with the XRD results.

3.3. AES characterization

Fig. 5 shows the parallel AES depth profiles of Ag, Cu, O and Ag, on the inner silver layer surface with adhered black oxides removed by the diamond

emery paper in sample A sintered for 1800 min. The parallel AES depth profiles of Ag and O on the outer silver layer surface are also shown. Fig. 6 shows AES spectra for 0 min sputtering and 18 min sputtering in Fig. 5(a), 20 min sputtering in Fig. 5(b). One can find from Fig. 5(a), an obvious oxygen-rich layer ($\sim$ 100 nm) and a copper-rich layer between Ag and the superconductor. Since the oxygen diffuses through Ag very rapidly (at 830°C, the oxygen diffusion coefficient in Ag is $D = 2.42 \times 10^{-5}$ cm^2/s) [28], a distance of 100 nm can be traversed in far below 1 min estimated as $(Dt)^{1/2}$. Therefore, the oxygen-rich layer can not be regarded as a diffusion layer. It results from the presence of the oxide contaminants in the sheath near the surface after the inner silver surface adhered with oxide has been slightly polished. Considering the observation of a copper out-diffusion layer by Hua et al. [29], the copper-rich layer may result from the presence of metallic contaminants followed by an out-diffusion layer of copper which is due to the very small diffusion coefficient of Cu in Ag (at 830°C $D = 5.4 \times 10^{-10}$ cm^2/s) [30]. After 6 min sputtering the Cu concentration curve oscillates with continuing of sputtering. It is because the Cu signal nearly disappears while the noise still exists, which is shown in Fig. 6(b). Fig. 5(b) shows the AES depth profile of Ag and O on another area of the same surface. It still shows an oxygen-rich layer resulting from the presence of the oxide contaminants. From Fig. 5(c), one can find that only an adsorbed O_2 layer exists on the outer silver layer surface. This suggests that the oxygen composition profiles in Fig. 5(a),(b) are not mainly contributed by the adsorbed O_2 during the preparation of the AES sample but by the oxide contaminants.

In the copper-rich layer, Bi, Pb, Sr, Ca are also rich. This can be seen from the AES spectra for 0 and 20 min sputtering as shown in Fig. 6. In the AES spectrum for 20 min sputtering there are no Bi, Pb,

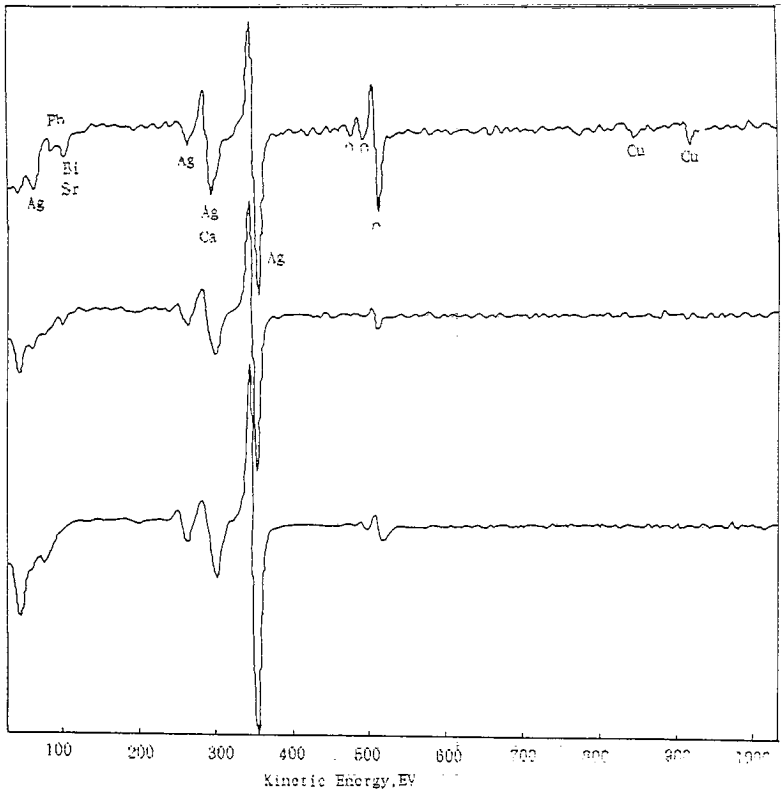

Fig. 6. AES spectra of silver layer sputtered for (a) 0 min, (b) 18 min in Fig. 5(a) and (c) 20 min in Fig. 5(b).

Sr, Ca and Cu signals, but there is still an O signal. The O signal is contributed by the oxygen dissolved in the silver. The oxygen dissolution equilibrium in Ag between 750 and 950°C has been studied [31]. The solubility of oxygen in solid Ag is given by [31]:

$$\tfrac{1}{2}O_2 = [O]_{Ag},$$

$$\Delta G^\circ = 48.150 - 16.41T\,(\mathrm{J/mol}),$$

$$K = [O]/P_{O_2}^{1/2} \text{ and } \Delta G^\circ = -RT \ln K,$$

$$[O] = P_{O_2}^{1/2}\exp(-\Delta G^\circ/RT). \quad (8)$$

Eq. (8) can be used to estimate the oxygen solubility in the sheath for our heat treatment conditions for which one calculates oxygen solubility of 1.73% at $T = 830$°C in air ($P_{O_2} = 0.21$ atm), which is nearly equal to the oxygen concentration after 20 min sputtering (Fig. 5(b)). Since the sample examined by AES is in quenched state and has been stored for two weeks, there may be a change of oxygen concentration distribution in the silver layer after quenching and storing, that is, the oxygen concentration will be very low in the outer silver surface as shown in Fig. 5(c), due to the oversaturation of oxygen in Ag at room temperature.

4. Discussion

4.1. Behavior of lead and oxygen during 2223 phase formation

Our results show that the removal of the lateral silver layers significantly affect the texture growth of the 2223 phase, i.e., simply existence of the broad silver layers is not enough to obtain the highly textured single 2223 phase. Another important finding is the existence of an oxygen enrichment layer on the contaminated inner silver layer. We should now first consider that the four configurations of the tapes, with various coverages of the core by the silver sheath, lead to a very important difference among the experiments, that is, the extent to which the lead in the core can volatilize. It is the easiest for Pb to volatilize at high temperature among the metallic elements in the BiPbSrCaCuO system [32,33].

As an effort similar to ours, Luo et al. [34] recently studied the effect of lead loss and sheath structure on phase formation and alignment in the Ag/Bi(2223) tape. They investigated two kinds of sheath structures, namely, an opened sample and a closed sample, corresponding to the samples B and A in our experiment, respectively. It was found that lead was the only metallic element to undergo substantial evaporation during annealing of the opened system for ~ 2 h at 825°C in 0.075 atm of oxygen, while for the closed sample, no detectable change in the stoichiometric balance of the metallic elements (including lead) even after annealing for up to 25800 min (430 h) under identical conditions. The Pb loss in the opened samples eventually caused a halt in the 2223 formation reaction from 1000 min annealing and a poorer texture, while the conversion to 2223 was completed within 1500 min (25 h) and a highly textured layer was formed in the closed sample.

Hornung et al. [35] investigated the effect of the atmosphere and the powder composition on the 2223 phase formation on two configurations of thick films prepared by combining the process of screen-printing with organic binders, cold deformation, and sintering. The two configurations are BiPbSrCaCuO/Ag (open system) and Ag/BiPbSrCaCuO/Ag (closed system), also corresponding to samples B and A in our study, respectively. They found that during annealing at 830–840°C, it was the Pb loss in the open system that resulted in slower 2223 phase formation and poorer degree of texture in the open system than in the closed system. They also claimed that to obtain a high content of 2223 phase in the open system, Ag or Ag_2O has to be added to the calcined powder and heat treatment has to be performed in an atmosphere containing PbO vapor.

Table 1 lists the composition normalized to Cu at different annealing stages for samples A, B, C and D. One can find that sample B experiences a significant decreases of Pb content to zero after annealing for 12000 min. However, the stoichiometry of Bi, Sr, Ca, Cu remained relatively constant, suggesting that those elements were less susceptible to high temperature evaporation than lead. This is consistent with the findings of Sata et al. [32] that the vapor pressure of lead over the BiPbSrCaCuO compound at 850°C in air was almost 2 orders of magnitude higher than that of Bi, Sr, Ca or Cu under the same conditions. However, sample A is subjected to nearly no Pb loss. Pb loss is slightly more obvious in samples C and D

Table 1
The composition normalized to Cu at different annealing stages for different samples

	Metal atom stoichiometry				
	Bi	Pb	Sr	Ca	Cu
Nominal composition	1.80	0.40	2.00	2.20	3.064
A					
12000 min	1.79	0.39	2.01	2.20	3.06
B					
100 min	1.75	0.38	2.00	2.21	3.06
12000 min	1.76	0.08	1.98	2.19	3.06
C					
200 min	1.78	0.39	2.00	2.19	3.06
12000 min	1.75	0.37	1.99	2.19	3.06
D					
250 min	1.78	0.39	1.99	2.21	3.06
12000 min	1.76	0.35	1.98	2.18	3.06

than in sample A and it is slightly more obvious in sample D than in sample C. Such a difference in the Pb loss between A, B, C and D is due to the fact that the coverage of the core by the silver sheath decreases in the sequence of A, C, D, and B. Considering the results of Luo et al. [33] and Hornung et al. [34], it seems reasonable that it is also the difference in the Pb loss that causes the differences in the rates of formation and texturing of the 2223 phase between samples A, B, C and D. That is, the less the exposed core is, the less Pb is lost. Without an adequate concentration of Pb, the 2223 phase will not readily form. Thus a lower Pb concentration leads to less 2223 phase and a poorer texture [33,34]. Therefore, the rates of formation and texturing of the 2223 phase decrease in the sequence of A, C, D and B.

The Pb contents in A, C, and D do not differ much from each other, although the Pb content slightly decreases in the sequence of A, C and D due to the decrease of the coverage of the core by the silver layer. This suggests that the broad silver layers act as the main barriers to prevent Pb evaporation. This point can also be supported by the fact that surface B + Ag shows a higher 2223 phase content than surface B (Fig. 2(a)). This is because surface B + Ag has more Pb than surface B due to the existence of the broad silver layer on surface B + Ag. So we can infer that most of the Pb in sample B is in the layer adjacent to the broad silver layer. In fact, there are always double open ends in the closed samples studied by Luo et al. [34] and Hornung et al. [35] and our sample A. Among these samples, the areas of the open ends are about 0.88, 0.12 and 0.48 mm^2, respectively, the areas of the double broad core surfaces are about 275, 120 and 180 mm^2, respectively, and the areas of the double lateral core surfaces are about 4, 1 and 4.8 mm^2, respectively. That is, the broad silver layer covers the largest areas of the core surface and thereby the Pb loss is mainly determined by whether the broad silver layer is removed. Neither the existence of open ends nor the removal of one or two lateral layers will result in an appreciable Pb loss.

However, the conversion to the 2223 phase and degree of texturing differ much from each other, decreasing in the sequence of A, C and D. The minor difference in Pb content between A, C and D may not be the only reason for the obvious differences in the conversion to the 2223 phase and degree of texturing. We thereby thought that the silver layer at least plays another role in texture growth of the 2223 phase besides the role that the silver sheath effectively prevents the evaporative lead loss and enhances the texture growth of the 2223 phase.

Zhu et al. [22] thought that the reaction among 2212 and Ca_2PbO_4, CuO to form the 2223 phase will produce O_2, i.e., $2212 + Ca_2PbO_4 + CuO \rightarrow 2223 + O_2$. If O_2 is formed during 2212 to 2223 phase transformation, it should be transported outward to promote further 2223 phase formation. The fact that the silver layer significantly promotes the formation and texturing of the 2223 phase lead us to believe that the silver layer can supply a favorable out-transport path for oxygen due to the stronger adsorption ability with respect to oxygen [36], the higher solubility of oxygen in Ag [31] and the greater diffusion coefficient of oxygen in Ag (at 830°C, $D = 2.42 \times 10^{-5}$ cm^2/s) [28]. Our AES results have shown that the oxygen out-diffusion through the silver sheath is very rapid, resulting in no oxygen enrichment layer at the Ag/core interface. The chemical diffusion coefficient of oxygen in the a–b plane of the 2212 phase at 830°C is 5.81×10^{-5} cm^2/s [37], namely about twice that in Ag. The

diffusion coefficient of oxygen in the a–b plane of the 2223 phase can be thought to be equal to that of the 2212 phase and the diffusion coefficients of oxygen in the c axis directions of the 2212 and 2223 phases are much smaller than those in the a–b plane directions of both phases [37]. If the oxygen diffuses outward toward the open ends, the diffusion distances in 50 and 200 h in the length direction which are estimated as $(Dt)^{1/2}$ are about 3 and 7 cm, respectively, which are much smaller than the length of a long tape, especially a kilometer-order long tape. However, the diffusion distances in 50 and 200 h in the silver sheath are about 2 and 4 cm, respectively, which are much larger than the thickness of the silver sheath (~ 0.035 mm in this study). Therefore if oxygen is formed during reaction to the 2223 phase, the most possible path for it to diffuse outward is the silver sheath. To investigate the reason why O_2 is produced during 2223 phase formation, we characterized the tape with XPS.

Fig. 7 shows the XPS spectra of Bi 4f, Pb 4f, Sr 3d, Ca 2p and Cu 2p of the broad surfaces on sample A sintered for 0 and 1800 min after the upper silver layer was peeled off. It should be stated first that the binding energy of the element in the 2212 structure is nearly identical to that in the 2223 structure due to the similar structure of both phases, which was observed in our experiment. No obvious chemical shift for the Bi 4f binding energy is found, suggesting that Bi exists in the 2212 crystal structure at 0 min and in both the 2223 and 2212 crystal structures at 1800 min, and no Bi-containing second phases are formed during the 2212 to 2223 phase transformation. For the Pb 4f spectrum of the green tape, two sets of obvious peaks exist, whose Pb $4f_{7/2}$ binding energies are 137.7 and 137.0 eV, corresponding to Pb in $(Ca,Sr)_2PbO_4$ and the 2212 phase, respectively. For the Pb 4f spectrum of the sintered tape, the intensity of the Pb $4f_{7/2}$ peak at 137.0 eV belonging to 2212 and 2223 increases and becomes larger than that at 137.7 eV belonging to $(Ca,Sr)_2PbO_4$ due to the formation of the 2223 phase. The intensity of the Pb $4f_{7/2}$ peak corresponding to $(Ca,Sr)_2PbO_4$ reduces, suggesting that $(Ca,Sr)_2PbO_4$ reacts with 2212 and other phases to form the 2223 phase.

For the Sr 3d spectrum of the green tape, only obvious Sr 3d peaks of Sr in $(Ca,Sr)_2PbO_4$ with the Sr $3d_{5/2}$ peak at 133.1 eV are seen, although the 2212 phase exists as a main phase in the green tape. Its preferential orientation with (001) planes, especially BiO(001) planes, parallel to the tape plane, resulting from the preferential cleavage between the weak BiO bilayers during deformation, causes the 2212 grains at the surface of the tape to mainly terminate with the BiO planes. This point has been verified by high resolution transmission electron microscopy (HRTEM) and scanning tunneling microscopy (STM) [38,39]. It is also supported by the strong Bi 4f signals in the tapes (Fig. 5(a)). Therefore, the Sr 3d peak of the 2212 phase is very weak in the XPS spectra and covered by that of $(Ca,Sr)_2PbO_4$ judged by the asymmetric peak shape. In the following it will be shown that the photoelectron peaks of Ca and Cu in the 2212 phase are also not obviously seen in the XPS spectra like that of Sr in the 2212 phase. For the Sr 3d spectrum of the sintered tape, the Sr $3d_{5/2}$ peak of the 2223 phase (131.8 eV) [40] becomes obvious due to the formation of the 2223 phase. For the Ca 2p spectrum of the green tape, two sets of Ca $2p_{3/2}$ peaks exist at 350.5 and 348.0 eV, corresponding to Ca in $(Ca,Sr)_2PbO_4$ and Ca_2CuO_3 or $(Ca,Sr)_{14}Cu_{24}O_{41}$, respectively. However, for that of the sintered tape, a new Ca $2p_{3/2}$ peak (345.1 eV) appears corresponding to Ca in the 2223 phase [40]. For the Cu 2p spectrum of the green tape, there are obvious Cu 2p peaks (937.2 eV for Cu $2p_{3/2}3d^{10}L$) of CuO [41] and those of $(Ca,Sr)_{14}Cu_{24}O_{41}$ (944.2 eV for Cu$2p_{3/2}3d^{10}L$) with a higher copper valence. For the Cu 2p spectrum of the sintered tape, Cu 2p peaks (933.0 eV for Cu$2p_{3/2}3d^{10}L$) of the 2223 phase appear [40] and those of CuO nearly disappear, suggesting that CuO is a main reactant for 2223 phase formation.

The above XPS results indicate that 2212 and Ca_2PbO_4, Ca_2CuO_3, CuO, $(Ca,Sr)_{14}Cu_{24}O_{41}$ react between each other to form the 2223 phase. Although some other parallel reactions may also happen, the former might be the dominant process as described elsewhere [42,43]. Moreover, that the binding energy of Pb 4f of the 2223 phase is lower than that of $(Ca,Sr)_2PbO_4$ may support that the valence of Pb in Ca_2PbO_4 (quadrivalent) is higher than that in the 2223 phase (about trivalent), consistent with the suggestion of Hegde and Ganguly [44] that the lead

enters the BiO planes of the 2212 or 2223 phase as Pb^{2+} to replace Bi^{3+} and stabilize the superconducting phase. Such a replacement may cause the depletion of oxygen in the BiO planes, i.e. the release of oxygen from the BiO planes, and alter the nature of the superstructure [45,46]. Also, from the Pb 4f XPS of the green tape, Pb may almost exist in $(Ca,Sr)_2PbO_4$, i.e. 2212 contains a very small amount

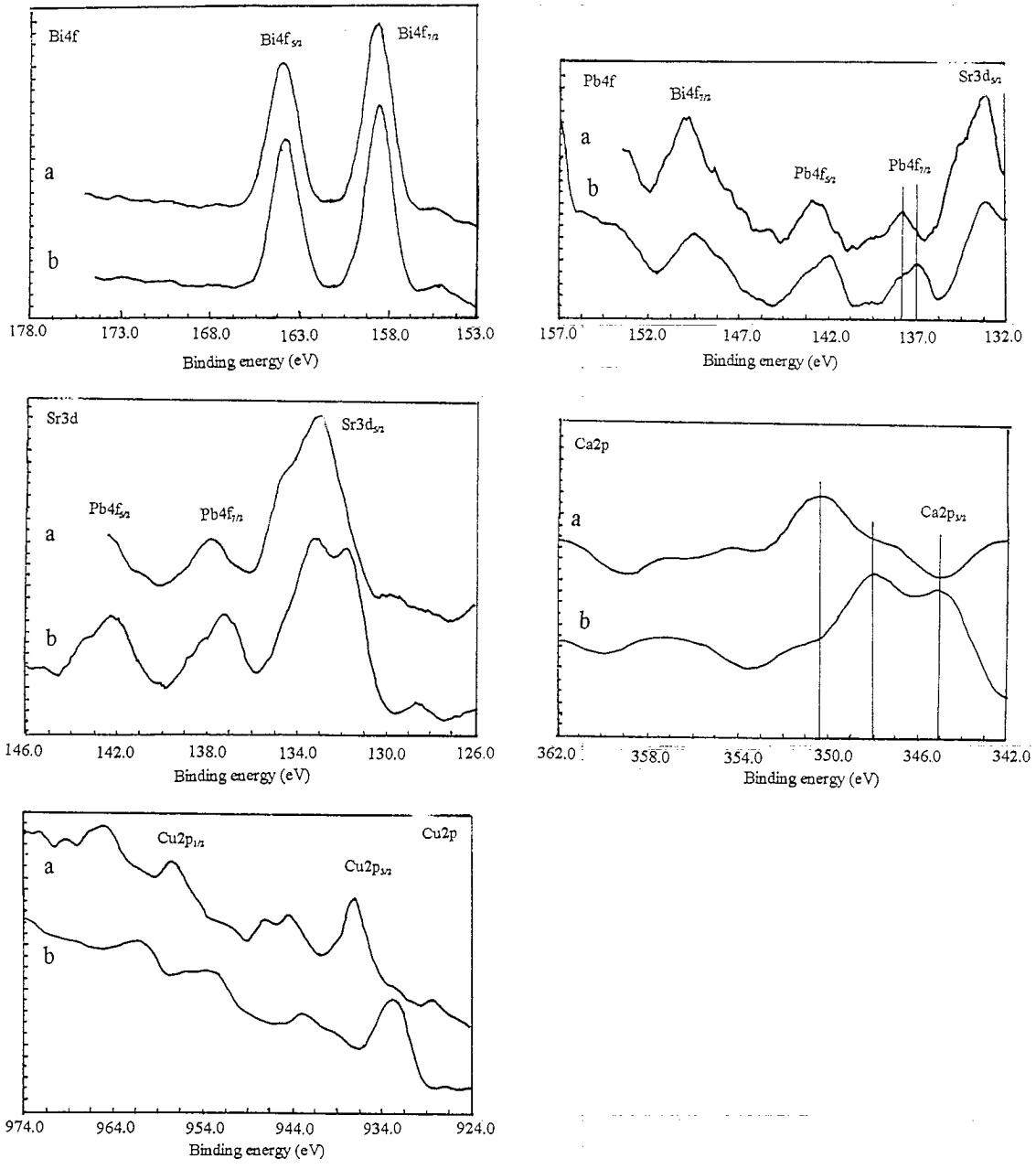

Fig. 7. Core level XPS spectra of Bi 4f, Pb 4f, Sr 3d, Ca 2p, Cu 2p of group A sintered for (a) 0 min and (b) 1800 min, respectively.

of Pb, although Dorris et al. [47] recently found that more complete 2223 formation was seen when all lead was incorporated in the 2212 phase rather than being added as either PbO or Ca_2PbO_4. So we can deduce that during the reaction between 2212 and Ca_2PbO_4, CuO, Ca_2CuO_3 $(Ca,Sr)_{14}Cu_{24}O_{41}$ to form the 2223 phase, lead (Pb^{4+}) released from Ca_2PbO_4 will enter into the BiO planes of 2212 as Pb^{2+} to stabilize the 2212 structure for further insertion of a $CaCuO_2$ layer to form the 2223 phase, accompanied by the oxygen release from the BiO planes due to the replacing of Bi^{3+} by Pb^{2+} [22,45,46]. The oxygen release during 2223 formation has been suggested in Ref. [22]. Such a release (oxygen valence from 2− to zero) happens to satisfy the charge balance during reaction, because of the accompanying valence reduction of Pb from 4+ in Ca_2PbO_4 to 2+ in 2223 and Cu from $2+\delta$ in $(Ca,Sr)_{14}Cu_{24}O_{41}$ to 2+ in 2223, there should be another element whose valence is increased [43]. It may be Cu in Ca_2CuO_3 or CuO for a cation because Ca and Sr are not elements with changeable valence while Bi does not show change valence from 2212 to 2223, or O for an anion. For Cu, the possible valence change is from 2+ in CuO or Ca_2CuO_3 to 3+ in 2223. But the cuprate superconductors are dominantly Cu(II) compounds. The Cu(III) state is formed to formally accommodate extra holes [48]. So the main possibility is that the valence of oxygen increases from 2− in 2212, $(Ca,Sr)_2PbO_4$, CuO or Ca_2CuO_3 to zero in gaseous O_2 during 2223 phase formation. Since Pb^{2+} enters into the BiO planes of the 2212 structure, the charge balance should be maintained in the BiO planes of the 2212 structure. Therefore, the gaseous O_2 is released from the 2212 phase. Thus the total formation process of the 2223 phase in our tape can be represented as:

$$2212(\text{Pb-poor}) + Ca_2PbO_4 + CuO + Ca_2CuO_3 + (Ca,Sr)_{14}Cu_{24}O_{41} \rightarrow 2223(\text{Pb-rich}) + O_2\uparrow. \quad (9)$$

Therefore, O_2 should escape in time to promote the 2223 phase formation in consistency with the thoughts proposed by Zhu et al. [22]. Otherwise there will be an increment of P_{O_2} in the tape, which further prohibits the 2223 phase formation.

4.2. Mass transport process of oxygen

Now another important question that needs to be clarified is how the produced O_2 escapes from the oxide core in the Ag/Bi(2223) tape to environment. Considering the AES results (Fig. 5) and the very long diffusion distance for oxygen along the length direction (namely towards the open ends) together with the fact that 2223 still forms when the length of tape is reduced to be much smaller than the width of the core [49], we propose that O_2 will be transported from the core through the silver layer to the environment. The mass transfer model can be described as a series of sequential steps as follows:

(1) Oxygen is produced during the reaction to the 2223 phase.

(2) Oxygen diffuses through the oxide layer to the inner silver layer surface.

(3) Oxygen adsorbs onto the inner silver layer surface at the Ag/core interface.

(4) The adsorbed oxygen dissolves into the silver layer surface at the Ag/core interface.

(5) The dissolved oxygen diffuses from the inner silver surface to the outer silver surface, namely the Ag/air interface.

(6) Oxygen escapes in gas state at the outer surface, i.e. the following reaction happens:

$$[O]_{Ag} = \tfrac{1}{2}O_2. \quad (10)$$

Because of the stronger adsorption ability of the silver layer with respect to oxygen [36], the higher solubility of oxygen in Ag [31] and the greater diffusion coefficient of oxygen in Ag [28], also, from the AES profiles (Fig. 5), the above oxygen mass transport is very rapid and so step (1) may be the rate limiting step. That is, as soon as oxygen is formed during reaction, it can be transported to the environment in time, and thus there will be no enrichment of oxygen in the core and the Ag/core interface, as shown in Fig. 5.

Otherwise, if the oxygen directly escapes from the oxide core, the following reaction happens:

$$[O]_s = \tfrac{1}{2}O_2 \quad (11)$$

where $[O]_s$ denotes the atomic oxygen in the oxide lattice because the short circuit diffusion will not be obvious at the high temperature with the formation of the dense textured oxide layer.

Now we can compare the possibilities of reactions (10) and (11) in terms of thermodynamics. The Gibbs free energy change (ΔG) of reactions (10) and (11) can be represented by:

$$\Delta G = \Delta G^\circ + RT \ln P_{O_2}^{1/2}/[O],$$

$$\Delta G^\circ = -RT \ln\left[(P_{O_2})_e\right]^{1/2}/[O]_e \qquad (12)$$

where ΔG° is the standard Gibbs free energy change, R the gas constant, T the absolute temperature, $(P_{O_2})_e$ the equilibrium partial pressure of O_2 at an oxygen concentration of $[O]_e$, P_{O_2} the actual partial pressure of O_2 in the environment, [O] the actual oxygen concentration in the silver for reaction (10) or oxide lattice for reaction (11).

Only when $\Delta G < 0$ reactions (10) or (11) can take place. That is,

$$\left[(P_{O_2})_e\right]^{1/2}/[O]_e > (P_{O_2})^{1/2}/[O]. \qquad (13)$$

Formula (13) shows that when $[O] = [O]_e$, the condition of $(P_{O_2})_e > P_{O_2}$ should be satisfied to drive reaction (10) or (11) to take place, that is, at a certain temperature and oxygen concentration, reaction (10) or (11) becomes spontaneous when the P_{O_2} in the environment is lower than the equilibrium P_{O_2} for that temperature and oxygen concentration. Tetenbaum et al. [50] studied oxygen stoichiometry, phase stability and thermodynamic behavior of lead-doped Bi-2223. They found that at $T = 815$°C (the highest temperature investigated by them), only when x in $(Bi,Pb)_2Sr_2Ca_2Cu_3O_x$ exceeded ~ 10.25, the partial pressure of oxygen in equilibrium with $(Bi,Pb)_2Sr_2Ca_2Cu_3O_x$ can become larger than P_{O_2} in air. That is, for $(Bi,Pb)_2Sr_2Ca_2Cu_3O_x$, only when $x > 10.25$ reaction (11) can happen. Although in this study, $T = 830$°C and the core is mainly $(Bi,Pb)_2Sr_2Ca_1Cu_2O_x$ at the early annealing stage and becomes mainly $(Bi,Pb)_2Sr_2Ca_2Cu_3O_x$ only after a long-time annealing, it may be understood from the above results that reaction (11) happens only after a larger x in 2212 or 2223 is reached. While for reaction (10) at $T =$ 830°C from Eq. (8), only when [O] in Ag becomes larger than 1.73%, can $((P_{O_2})_e$ in reaction (10) become larger than that in air. A value of $[O]_{Ag} = 1.73\%$ can be achieved soon after temperature reaches 830°C. When the tape is slowly heated to 830°C at 1.5°C/min, the silver sheath will quickly dissolve oxygen. After the temperature reaches 830°C (no 2223 phase formation at this time), the equilibrium oxygen concentration will be 1.73% calculated from Eq. (8). When 2223 begins to form, the produced O_2 will make P_{O_2} in the sheath higher than that in the environment and then be dissolved in the silver sheath followed by diffusion through the sheath to the outer surface. Hence the $[O]_{Ag}$ becomes higher than its equilibrium value at the outer surface, which drives reaction (10) to happen. That is, as soon as the 2223 phase is formed, the produced oxygen will be transported outward through the silver layer quickly. The above comparisons further show that the oxygen transport through the Ag sheath and reaction (10) is more advantageous for 2223 formation. Moreover, the diffusion distance estimated as $(Dt)^{1/2}$ is 3 cm (the length of the core) in 50 h in the core towards the open ends assuming that the core is the textured 2212 phase, and is 0.0035 cm (the thickness of the sheath) in 0.5 s in the silver layer. Such calculations further support the above points of view.

Therefore, we can understand that it is just the oxygen release through reaction (10) instead of reaction (11) that makes the possibility of fabricating the silver-sheathed tapes at temperatures (820–840°C in air) lower than fabricating the bulk materials (840–860°C in air).

During the early stage of the 2223 phase formation, step (2) is not necessary because the produced O_2 can be directly adsorbed onto and further dissolved into the inner silver surface without diffusion through the oxide core layer in the atomic state. When a highly textured dense 2223 layer is formed, the O_2 formed in the inner oxide layer adjacent to the 2223 layer but closer to the center of the core has to first diffuse through the outer 2223 layer, i.e., step (2) is essential for 2223 phase formation. It may just be another reason why 2223 phase formation occurs preferably at the Ag/oxide interface [12–14] that the diffusion distance before reaching the inner silver surface is shortest for oxygen produced in the oxide layer near the Ag/oxide interface, besides the explanation that silver can interact with the oxide to form a liquid helpful for diffusion-controlled 2223 phase formation [15–18].

The longitudinal mass transport towards the open ends, i.e., not through the silver sheath, is not considered in the above mass transport model is for two main reasons. First, the longitudinal length is largest, especially for the kilometer-order long Ag/Bi(2223) tape. If the oxygen diffuses predominantly longitudinally towards the open ends, the rate of the 2223 phase formation in a long tape will be much slower than that in a short tape. Second, there is also complete 2223 phase formation in 200 h at 830°C when the longitudinal length is reduced to 1 mm (i.e. shorter than the width) [49].

To support the above proposed model, the model is used to explain why there exists an optimal P_{O_2} for 2223 phase formation in the Ag/Bi(2223) tape [21]. According to our model, it is not easy for step (5), i.e., reaction (10) to carry out towards right when P_{O_2} in the atmosphere is too high, and thereby the formation of the 2223 phase is not favored. But when the P_{O_2} in the atmosphere is too low, the 2223 phase becomes thermodynamically instable [46,50, 51].

One issue is how the oxygen behavior is when the precursor powder in the sheath contains no Ca_2PbO_4 but other non-superconducting phases such as Ca_2CuO_3, CuO besides the Pb-doped 2212 phase. The newest results show that Ca_2PbO_4 forms at temperatures well below the temperature where the 2223 phase is grown [52] or appears during the 2212 to 2223 phase transformation [53] when the precursor powder contains no Ca_2PbO_4. However, it can not be concluded that the 2223 phase formation is always related to the participation of Ca_2PbO_4. So one can not now infer that the Ag/Bi(2223) tape depends on P_{O_2} in a similar way when its precursor powder contains no Ca_2PbO_4, for example, when the phase mixture is Pb-doped 2212 + Ca_2CuO_3 + CuO. The study to investigate this point is now underway.

4.3. Mechanism of silver-induced texture

Many researchers have observed that the broad silver layer can promote formation and texturing of the 2223 phase [12–14], but no explicit physical model has been presented to explain this phenomenon. Furthermore, to our knowledge, no authors except us have found that even the lateral silver layers play an important role in the texture growth of the 2223 phase in the Ag/Bi(2223) tapes. Luo et al. [34] and Hornung et al. [35] claimed that the role of silver sheaths is to prevent Pb loss during high temperature reaction to the 2223 phase and to enhance the formation and texturing of the 2223 phase. However, no large difference in the Pb loss between samples A, C and D is found while great differences in the formation and texturing of the 2223 phase are confirmed. Our results show that the Pb loss is mainly controlled by the broad silver layer due to the largest area fraction of the broad surface in the thin Ag/Bi-2223 tape. If two broad surfaces are present, no large difference in Pb loss is found (e.g. A, C, D). If one broad silver layer is removed, the non-exposed broad core surface still contains the 2223 phase (e.g. B + Ag). So it can not be thought that to prevent the lead loss is the only role of the silver layer. Some researchers [12–18] thought that the role of the silver layer is to preferably induce liquid formation at the Ag/core interface and hence to promote formation and texturing of the 2223 phase. But this understanding of the role can not answer why even the removal of the lateral silver layers affects the texture growth of the 2223 phase, Also, the strong dependence of the 2223 phase formation on P_{O_2} in the sheath [21] and our AES and XPS results firmly indicate that the 2223 phase formation is related to oxygen release. According to our described oxygen mass transport process, the inherent mechanism of the silver-induced texture (SIT) can be discussed in more detail.

That is, the role of the silver sheath is a combination of prevention of the Pb loss, supplying a fast out-diffusion path, inducing of liquid, and acting as a quasi-two-dimensional space.

(1) The silver layer promotes 2223 formation by prevention of the Pb loss at high temperatures to maintain an adequate Pb concentration, supplying a fast out-diffusion path for oxygen produced during reaction, and interaction with oxide to form liquid to accelerate atomic diffusion [15–18], and thereby supplying more 2223 grains to be textured by the RIT mechanism. Therefore, the more readily the 2223 phase forms, the more readily the texturing develops.

(2) The broad silver layers preferably promote nucleation and growth of the 2223 phase with the a–b plane parallel to the tape plane and suppress the

non-oriented grain growth of the 2223 phase. Because the a–b planes of the non-textured 2223 phase grains will quickly meet the textured 2223 phase grains or a broad silver layer due to the faster growth in the a–b plane direction than in the c-axis direction and thereby the non-oriented grain growth will be quickly impeded [54].

(3) The lateral silver layers preferably supply an out-diffusion path of oxygen for the formation of the preferably oriented 2223 phase. That is why only removal of one or both lateral silver layers (sample C or D) also affects the degree of texture of the 2223 phase while the Pb contents are nearly same in A, C, D (Fig. 2 and Table 1). This can be explained by the oxygen mass transport model described in Section 4.2. When the lateral silver layers are removed, only the a–b plane of the non-textured 2223 grains are clinically in intimate contact with the silver layer and hence it is easy for oxygen to escape in the fashion of reaction Eq. (10). However, the a–b planes of the textured 2223 grains do not intersect with the broad silver layer and thus the oxygen produced by formation of the textured 2223 phase can not quickly escape in the a–b plane directions and mainly escape in the c directions, i.e. oxygen diffuses through the silver layer to the broad silver layer surface and chemically escapes in the fashion of reaction Eq. (10). Because the diffusion of oxygen in the c direction is much slower than that in the a–b plane direction [37], relatively, the non-textured 2223 grains are more favored to form due to the easier release of as-formed oxygen than the textured 2223 grain. Thus the degree of texture in the tape with the lateral silver layers removed is lower than that in the tape without any part removed, and that in the tape with both the lateral silver layers removed is lower than that in the tape with one lateral silver layer removed.

It shows that the key to form a highly textured 2223 phase is the existence of both the broad silver layers and the lateral silver layers. The former can prevent the Pb loss and preferably supply a quasi-two-dimension configuration for the textured 2223 grain growth while the latter can preferably supply a fast out-diffusion path of oxygen for textured 2223 grain formation. Both can induce liquid formation. Not only the easy release of the oxygen during 2223 phase formation, and the excellent growth space for textured 2223 phase growth, and the prevention of the Pb loss, but also the inducing of liquid, enhance the texture growth of the 2223 phase.

For surface B, the substantial Pb loss, the slow oxygen release and the inexistence of liquid related to silver cause the very slow 2223 phase formation and the impedance for non-oriented grain growth by the broad silver layer does not exist. Therefore, the texturing process is slowed down. For surface B + Ag, the existence of the broad silver layer causes less Pb loss, faster oxygen release suppression of the non-oriented grain growth and the existence of liquid induced by the broad silver layer compared to surface B, and thereby more 2223 phase with a higher degree of texture is formed at surface B + Ag than at surface B. For surface A, formation and texturing of the 2223 phase are promoted by the maintenance of Pb, fast release of oxygen, existence of liquid and suppression of non-oriented grain growth. Compared to surface A, for surfaces C and D, one or two favorable directions in which the oxygen produced during the textured 2223 grain formation preferably diffuses will not exist. Hence the release of oxygen is slower, the local P_{O_2} in the sheath is higher, which in turn lowers the rate of 2223 phase formation and thereby, relatively, there will be less 2223 grains to be textured, resulting in the lower degree of texture than surface A.

5. Conclusion

During 2212 to 2223 phase transformation, oxygen will be released from the BiO planes of 2212 to compensate the valence reduction of Pb after Pb^{4+} enters the BiO plane of 2212 as Pb^{2+} to make 2223 nucleate. The silver layer just supplies a favorable out-diffusion path for the produced oxygen to escape in time and thereby promotes 2223 phase formation. The silver sheath, especially the broad layer, effectively prevents Pb loss to maintain an adequate Pb concentration for 2223 formation.

The mechanism of silver-induced texture (SIT) is a combination of preventing the Pb loss by the silver sheath, supplying a fast out-diffusion path for the oxygen produced during 2212 to 2223 transformation, inducing liquid to accelerate 2223 formation, and acting as quasi-two-dimensional growth space for the textured 2223 grains. The former three factors promote the SIT through enhancing 2223 phase for-

mation, and hence supply more 2223 grains to be textured by the RIT mechanism. The second factor also acts through preferably supplying the out-diffusion path of oxygen for formation of preferably oriented 2223 phase grains, due to the anisotropy of oxygen diffusion in the layered superconducting phase. When the core is wrapped by the sheath, all the factors contribute to promoting the formation and texturing of the 2223 phase. When one or more parts of the sheath are removed, that is, lateral layers or broad layers or both, one or more factors will not exist, which in turn reduces the rates of formation and texturing of the 2223 phase. When the broad layer is removed, 2223 phase formation will finally stop due to the escape of nearly all the Pb.

References

[1] S. Jin, J. Graebner, Mater. Sci. Eng. B 7 (1991) 243.
[2] C.L. Briant, E.L. Hall, K.W. Lay, J.E. Tkaczyk, J. Mater. Res 11 (1994) 2789.
[3] Y. Feng, Y.E. High, D.C. Larbalestier, Y.S. Sung, E.E. Hellstrom, Appl. Phys. Lett. 62 (13) (1991) 1553.
[4] N. Merchant, J.S. Luo, V.A. Maroni, G.N. Riley Jr., W.L. Carter, Appl. Phys. Lett. 65 (6) (1994) 1039.
[5] P.S. Mukherjee, J. Koshy, A. Simon, P. Guruswamy, A.D. Damodaran, Solid State Commun. 6 (1990) 477.
[6] G. Grasso, A. Perin, R. Flukiger, Physica C 250 (1995) 43.
[7] Y.C. Guo, H.K. Liu, S.X. Dou, J. Mater Res. 9 (1993) 2187.
[8] Y. Yamada, B. Obst, R. Flukiger, Supercond. Sci. Technol. 4 (1991) 165.
[9] M. Wilhelm, H.W. Neumuler, G. Reis, Physica C 185-189 (1991) 2399.
[10] J.S. Luo, N. Merchant, V.A. Maroni, G.N. Riley Jr., N.L. Carter, Appl. Phys. Lett. 63 (5) (1993) 690.
[11] Y. Feng, D.C. Larbalestier, Interf. Sci. 1 (1994) 401.
[12] M. Satou, Y. Yamada, S. Nurase, T. Kitamure, Y. Kamisada, Appl. Phys. Lett. 64 (5) (1994) 640.
[13] Y. Feng, Y.E. High, D.C. Larbalestier, Y.S. Sung, E.E. Hellstrom, Appl. Phys. Lett. 62 (1993) 1553.
[14] Y.E. High, Y. Feng, Y.S. Sung, E.E. Hellstrom, D.C. Larbalestier, Physica C 220 (1994) 81.
[15] H.K. Liu, S.X. Dou, Z.B. Shao, K.R. Liu, L.Q. Liu, J. Supercond. 7 (10) (1994) 69.
[16] S.X. Dou, Y.C. Guo, K.K. Nang, M. Ionescu, H.K. Liu, E. Babic, I. Kusevic, IEEE Trans. Appl. Supercond. 52 (2) (1995) 1830.
[17] P.E.D. Morgan, R.M. Housley, J.R. Porter, J.J. Ratto, Physica C 176 (1991) 279.
[18] J.S. Luo, N. Merchant, E. Escorcia-Aparicio, V.A. Maroni, D.M. Gruen, B.S. Tani, G.N. Riley Jr., W.L. Carter, IEEE Trans. Appl. Supercond. 3 (1993) 972.
[19] J. Kang, X. Chen, Y. Wang, R. Han, G. Xiong, G. Liang, J. Li, R. Wu, Solid State Commun. 2 (1995) 99.
[20] J. Guo, J.A. Lewis, K.C. Goretta, J. Schwartz, J. Appl. Phys. 78177 (1995) 4596.
[21] K. Fischer, M. Schubert, C. Rodig, P. Verges, H.W. Neumuller, B. Koas, A. Jenovelis, IEEE Trans. Appl. Supercond. 5 (2) (1995) 1259.
[22] W. Zhu, P.S. Nicholson, J. Appl. Phys. 73 (1993) 8423.
[23] D.C. Larbalestier, X.Y. Cai, Y. Feng, H. Edelman, A. Umezawa, G.N. Riley Jr., W.L. Carter, Physica C 221 (1994) 299.
[24] M. Lelovic, P. Krichnaraj, N.G. Eror, U. Balachandran, Physica C 242 (1995) 246.
[25] U. Welp, D. Gunter, G. Crabtrae, W. Zhang, U. Balachandran, P. Haldar, R. Sokolowski, V. Vlasko-Vlasov, V. Nikitenko, Nature (London) 376 (1995) 144.
[26] S. Hofmann, Surf. Interf. Anal. 2 (1980) 148.
[27] M.P. Seah, Thin Solid Films 81 (1981) 279.
[28] W. Eichenauaer, G. Muller, Z. Metallkd. 53 (1962) 321.
[29] L. Hua, Q.Z. Yao, M. Tiang, Y.Z. Wang, H. Tang, Z.R. Li, G.W. Qiao, J. Appl. Phys. 78 (5) (1995) 3274.
[30] J.R. Cahoon, W.V. Youdelis, Trans. Met. Soc. AIME 239 (1967) 127.
[31] T.A. Ramanarayanan, R.A. Rapp, Met. Trans. 3 (1972) 3239.
[32] T. Sata, K. Sakai, S. Tashiro, J. Am. Ceram. Soc. 75 (1992) 805.
[33] T.W. Button, N.McN. Alford, J.D. Birchall, F. Wellofer, C.E. Gough, D.A. O'Connor, Supercond. Sci. Technol. 2 (1989) 224.
[34] J.S. Luo, N. Merchant, V.A. Maroni, S.E. Dorris, M.T. Lanagan, B.S. Tani, J. Am. Ceram. Soc. 78 (1995) 2785.
[35] R. Hormung, H.W. Neumuller, M. Wilhelm, G. Tomadl, J. Mater. Res. 9 (1994) 1967.
[36] P.A. Kilty, N.C. Rol, W.M.H. Sachlter, Proc. 5th Intern. Congr. Catalysis, FL, 1973, p. 929.
[37] J.L. Routbort, S.J. Rothman, J. Appl. Phys. 76 (1994) 5615.
[38] C.K. Shih, R.M. Feenstra, J.R. Kirtley, G.V. Chandrashekhar, Phys. Rev. B 40 (1989) 2682.
[39] M. Tanaka, T. Takahashi, H. Katayama-Yoshida, S. Yamazaki, M. Fujinami, Y. Okabe, W. Mizutani, M. Ono, K. Jijimura, Nature 339 (1989) 691.
[40] S.U. Woo, H.K. Duk, N. Kwangsoo, G.K. Ho, Jpn. J. Appl. Phys. 31 (3) (1992) 77529.
[41] M. Ji, Z. He, J. Wu, H. Zhang, G. Pan, Z. Cheng, Y. Qian, Y. Zhao, L. Hu, J. Xia, Q. Zhang, Solid State Commmun. 63 (6) (1987) 511.
[42] G.M. Zorn, R. Hornung, N.E. Gobel, B. Seebaoher, H.W. Neumieller, G. Tomandl, Supercond. Sci. Technol. 8 (1995) 234.
[43] M.G. Smith, D.S. Phillips, D.E. Peterson, J.Q. Willis, Physica C 224 (1994) 168.
[44] M.S. Hegde, P. Ganguly, Phys. Rev. B 38 (1988) 4557.
[45] R. Ramesh, G.V. Tendeloo, G. Thomas, S.M. Green, H.L. Luo, Appl. Phys. Lett. 53 (1988) 2220.
[46] S.M. Green, Y. Mei, A.E. Manzi, H.L. Luo, J. Appl. Phys. 66 (1989) 3703.

[47] S.E. Dorris, B.C. Prorok, M.T. Lanagan, N.B. Browning, M.R. Hagen, J.A. Paraell, Y. Feng, A. Umezawa, D.C. Larbalestier, Physica C 223 (1994) 163.
[48] R.E. Egdell, W.R. Flavell, M.S. Golden, Supercond. Sci. Technol. 3 (1990) 8.
[49] C.B. Mao, L. Zhou, X.Y. Sun, X.Z. Wu, Supercond. Sci. Technol., in press.
[50] M. Tetenbaum, M. Hash, B.S. Tani, J.S. Luo, V.A. Maroni, Physica C 249 (1995) 396.
[51] J.L. Macmanus-Driscoll, J.C. Brarman, R.J. Savery, G. Gorman, R.B. Beyers, J. Am. Ceram. Soc. 77 (9) (1994) 2305.
[52] Ming Xu, D.K. Finnemore, U. Balachandran, P. Haldar, Appl. Phys. Lett. 66 (24) (1995) 3359.
[53] C.K. Sang, G.Z. Hee, T.A. Byung, W.N. Soo, Supercond. Sci. Technol. 7 (1995) 552.
[54] T.D. Aksenova, P.V. Bratukhin, S.V. Sharkin, V.L. Melnikov, E.V. Antipova, N.E. Khlebova, A.K. Shikov, Physica C 205 (1993) 271.